Condensed Matter Physics, 2005, Vol. 8, No. 2(42), pp. 1–??

CONDENSED MATTER PHYSICS

Nonequilibrium molecular dynamics

Wm.G.Hoover, C.G.Hoover

Highway Contract 60, Box 565, Ruby Valley, Nevada 89833,
Department of Applied Science University of California
at Davis/Livermore and Lawrence Livermore National Laboratory,
Livermore, California 94551–7808.

Received February 16, 2005

Nonequilibrium Molecular Dynamics is a powerful simulation tool. Like its equilibrium cousin, *nonequilibrium* molecular dynamics is based on *time-reversible* equations of motion. But unlike conventional mechanics, nonequilibrium molecular dynamics provides a consistent microscopic basis for the irreversible macroscopic Second Law of Thermodynamics. We recall here how fast computers led to the development of nonequilibrium molecular dynamics from the statistical mechanics of the 1950s. Computer-based theories facilitated revolutionary breakthroughs in understanding during the 1970s and 1980s. The new idea key to the *nonequilibrium* development was the replacement of the *external* thermodynamic environment by *internal* control variables. The new variables can control temperature, or pressure, or energy, or stress, or heat flux. These thermostat, barostat, ergostat, ... variables can control and maintain *nonequilibrium* states. We illustrate the methods with a simple example well-suited to student exploration, a thermostatted harmonic oscillator exposed to a temperature gradient.

Key words:

PACS:

1. Introduction

David Barash's invitation to celebrate Doug Henderson's 70th Birthday in Utah was welcome for many reasons. Besides the social and scientific values there was the chance to visit a part of the West near our home-building project in Ruby Valley, Nevada. The Interstate Highway System facilitated Bill's visit to honor Doug at Brigham Young University in Provo while Carol tended the horses, cats, and computers in and around our homes in California.

Doug is an "old" friend in more ways than one. His work in equilibrium statistical mechanics, in the 1960s, was along similar lines to Bill's. There were plenty of opportunities for getting together for discussions: Gordon conferences, the annual West Coast Statistical Mechanics meetings, and social and scientific visits at our various Bay Area homes and workplaces.

The present report summarizes our progress since then, progress in understanding *nonequilibrium* statistical mechanics following the development of nonequilibrium molecular dynamics. The work described here spans roughly the interval between Doug's 40th and 70th birthdays. We wish him another such interval!

We sketch the main ideas here in an informal way. The detailed arguments and literature references can be found in the references, supplemented, for the most recent work, by a diligent internet search. While our supply lasts, we would be happy to mail a copy of Bill's book, "Time Reversibility, Computer Simulation, and Chaos" [1], to any interested readers desiring more details. An earlier (1991) book [2] "Computational Statistical Mechanics", is available in pdf form at our website: http://williamhoover.info.

2. Equilibrium statistical mechanics

Statistical mechanics undertakes the explanation of macroscopic thermodynamic and hydrodynamic behavior in terms of underlying microscopic models. All the equilibrium behavior (radial distribution functions, equations of state, phase diagrams, ...) of these models follows from Gibbs' and Boltzmann's 1883 idea of replacing time averages by phase-space averages: a properly weighted (q,p) phase-space average can provide the same information as a long-time-averaged dynamical simulation.

The "materials" treated by statistical mechanics are mechanical models, prescriptions for the motion of microscopic masses. The simplest models are described by a Hamiltonian $H = K + \Phi$ with a momentum-dependent kinetic energy K and a coordinate-dependent potential Φ. Hamilton's equations of motion describe the corresponding dynamics in terms of first-order differential equations of motion.

$$H(q,p) = \Phi(q) + K(p) \longrightarrow \quad \{\dot{q} = +\partial H/\partial p = \partial K/\partial p = p/m\} \; ; \quad \{\dot{p} = -\partial H/\partial q = -\partial \Phi/\partial q = F(q)\} \; .$$

Numerical solutions of Hamilton's equations can be obtained using the Runge-Kutta method. In numerical work the product of the number of (q,p) degrees of freedom and the number of timesteps is limited to about 10^{12}.

A theoretical analysis of Hamilton's equations has a fundamental consequence for the equilibrium statistical mechanics of isolated systems. In this case the probability density $f(q,p,t)$ is necessarily stationary at any fixed phase-space location: $\partial f/\partial t = 0$, implying that the density must also be stationary *following the flow*, $\mathrm{d}f/\mathrm{d}t = 0$. *Liouville's Theorem* (that a phase-space probability density governed by Hamiltonian mechanics flows through the space with unchanging density, like an incompressible fluid) implies that the stationary solution must necessarily have the same constant value throughout all the mutually-accessible parts of phase space:

$$\mathrm{d}f/\mathrm{d}t = 0 \longrightarrow f(q,p) = \text{ constant.}$$

The time derivative following the flow, $\mathrm{d}f/\mathrm{d}t$, is necessarily zero as a direct consequence of the motion equations, leading to the conclusion that f has the same value at any state accessible from the initial conditions placed on the flow.

The resulting constant-density distribution of states is Gibbs' "microcanonical" ensemble. There is an important special case. In the event that a part of the system is an ideal-gas thermometer the equilibrium phase-space distribution is a product,

$$f(q,p) = f_{\rm ideal} \times f_{\rm other}\,.$$

In this special case, the entropies, $S = -k \ln f$ are additive, and entropy maximization (the definition of the equilibrium situation) establishes that the temperatures,

$$T_{\rm ideal} = \langle p^2/mk \rangle_{\rm ideal}\,, \qquad T_{\rm other} = \langle p^2/mk \rangle_{\rm other}$$

and pressures are equal too, and that the distribution $f_{\rm other}$ is Gibbs' "canonical" distribution:

$$f_{\rm other} \propto \exp[-H_{\rm other}(q,p)/kT], \qquad T = T_{\rm ideal} = T_{\rm other}\,.$$

The identification of the macroscopic thermodynamic concepts of entropy and temperature with microscopic properties of a stationary distribution is the most significant result of Gibbs' and Boltzmann's work.

The canonical distribution then leads to all the usual textbook statistical mechanics, relating all the macroscopic equilibrium properties (including the Green-Kubo expressions for the transport coefficients) to microscopic averages. The main catch is that the microscopic expressions, integrals in $6N$-dimensional (q,p) "phase space" or $3N$-dimensional (q) "coordinate space", are just as hard to evaluate as are many-body dynamical averages.

From the 1930s through the 1950s a widespread theoretical effort sought ways to simplify the evaluation of microscopic phase-space averages. The Mayers' virial series provided density expansions around the low-density (ideal gas) limit. Einstein models and cell models provided higher-density approximations. Integral equations (for the pair distribution function) provided approximate approaches of uncertain validity over a wide density range.

In the 1950s a new approach began to render these older ways obsolete. Fermi, Alder, and Vineyard, along with many coworkers, developed molecular dynamics, going back to the idea of time averages and using fast computers to solve the many-body dynamics. Bill Wood and his coworkers at Los Alamos developed Metropolis', the Rosenbluths', and the Tellers' Monte Carlo method for phase-space averages. Comparisons showed that the old Gibbs-Boltzmann approach was indeed correct. Time averages and phase averages agreed.

Even though it was possible to solve equilibrium problems by direct simulation(molecular dynamics and Monte Carlo were about equally costly) it was desirable to save time/money by relating new problems to old solutions. "Perturbation theory", based on the computer results (free energy and radial distribution function) for "reference systems", allowed accurate estimates of thermodynamic properties. Such theories were developed by several different groups. John Barker, Doug Henderson, and George Stell were in the forefront of this effort. The result of their labors was to finish off the problem of finding thermodynamic properties using equilibrium

statistical mechanics. A fringe benefit was the opening up of interest in *nonequilibrium* problems, a subject which has kept us occupied for the past 30 years. The high spots of this nonequilibrium effort are what we emphasize here in this paper honoring Doug and the happy occasion of his 70th birthday.

3. Motion equations for nonequilibrium molecular dynamics

The equilibrium identification of macroscopic temperature with the microscopic kinetic energy made it natural to constrain or control the temperature of a many-body system by "rescaling" the kinetic energy. If the temperature was too low or too high it could be adjusted by multiplying all the velocities by a common velocity-rescaling multiplier. Though it was not realized at the time, a continuous version of this rescaling procedure satisfies the simple differential equations of motion:

$$\begin{aligned} \{m\ddot{q} &= \dot{p} = F(q) - \zeta p = F(q) - \zeta m\dot{q}\}, \\ \zeta &= \sum F\cdot p / \sum p^2 = \sum F\cdot \dot{q} / \sum m\dot{q}^2, \\ &\longrightarrow \mathrm{d}K/\mathrm{d}t = \sum p\cdot\dot{p}/m = \sum p\cdot(F-\zeta p)/m \equiv 0. \end{aligned}$$

The "friction coefficient" (or "control variable") ζ is positive whenever the forces $\{F\}$ are acting to increase the kinetic energy, and negative whenever the forces would cause the kinetic energy to decrease. ζ keeps the kinetic energy (temperature) of the system strictly constant.

Of course there are other possibilities for equations of motion controlling kinetic energy. A constraint force varying as p^3 or p^5 could be used. Why should the "right" constraint force be *linear* in the momenta? There is a long-standing principle in mechanics, Gauss' Principle of Least Constraint, stating that constraints should be applied with the smallest possible (in the least-squared sense) constraint forces:

$$\{\dot{p} = F + F_{\rm c}\}, \qquad \sum F_{\rm c}^2/m \text{ a minimum.}$$

When this least-constraint principle is applied to the problem of constraining the kinetic temperature the solution,

$$\{F_{\rm c} = -\zeta p\}, \qquad \zeta = \sum F\cdot p / \sum p^2$$

is identical to the motion equations obtained above with velocity rescaling.

In a remarkable generalization of these simple ideas, Shuichi Nosé [3] showed that a friction coefficient based on integral feedback:

$$\begin{aligned} \dot{\zeta} &= \sum \left[\left(p^2/mkT \right) - 1 \right] / \#\tau^2 \rightarrow \\ \zeta(t) &= \zeta(0) + \int_0^t \sum \left[\left(p^2/mkT \right) - 1 \right] \mathrm{d}t' / \#\tau^2 \ , \end{aligned}$$

was fully consistent with Gibbs' canonical distribution for # thermostatted degrees of freedom, each with mass m. Here τ is a relaxation time, the characteristic time

required to control temperature fluctuations. In this approach the kinetic energy fluctuates, and in just such a way as to trace out the canonical distribution over time. The friction coefficient consistent with Gibbs' distribution has a Gaussian distribution:

$$f(q, p, \zeta) \propto \exp(-H/kT) \exp(-\#\zeta^2\tau^2/2).$$

Nosé based his development on Hamiltonian mechanics, through two special Hamiltonians which lead directly to the friction-coefficient equations of motion. This Hamiltonian basis guarantees their time-reversible nature. Time reversibility implies that any movie of a motion satisfying the equations will also satisfy them if the frames are projected in reversed order. It is an interesting excercise to show that the "Nosé-Hoover" equations $m\ddot{q} = F - \zeta m\dot{q}$ result from the better of Nosé's two Hamiltonians:

$$H_{\text{Nosé}} = (K/s) = s\left[\Phi + (p_s^2/2M) + \#kT \ln s\right] = 0,$$

where the "mass" M associated with the action variable p_s is $\#kT\tau^2$.

It is somewhat simpler to develop Nosé's ideas (as well as their generalizations to constant-stress or constant-strain ensembles) by (i) *assuming* a constraint force linear in the momenta, $F_{\text{C}} = -\zeta p$ and then (ii) using the corresponding form of Liouville's Theorem [4] to evaluate the change of f in time for the resulting compressible phase-space flow:

$$\begin{aligned} \partial f/\partial t &= \sum \left[-\partial(f\dot{q})/\partial q - \partial(f\dot{p})/\partial p\right] - \partial(f\dot{\zeta})/\partial\zeta, \\ \mathrm{d}\ln f/\mathrm{d}t &= \sum \zeta. \end{aligned}$$

Adding the further requirement (iii) that the resulting f have Gibbs' equilibrium form results again in the "Nosé-Hoover" form of Nosé's feedback equation:

$$\dot{\zeta} = \sum \left[(p^2/mkT) - 1\right]/\#\tau^2.$$

The new motion equations, with their control variables, made it possible to constrain temperature or pressure or energy for selected degrees of freedom. The constraints could also be generalized to apply locally, in either space or time. In the equilibrium case, with temperature and pressure uniform, all the results of statistical mechanics were reproduced and recovered. We turn next to the consequences of the new dynamics *away* from equilibrium.

4. Results from nonequilibrium molecular dynamics

Many-body diffusive flows, viscous flows, and heat flows were all simulated in the 1970s. By 1990 million-particle systems had been simulated. A sample appears in figure 1. In that work we simulated the plastic indentation of silicon (using the Stillinger-Weber many-body potential) and found a yield stress in good agreement with experimental data for silicon [5].

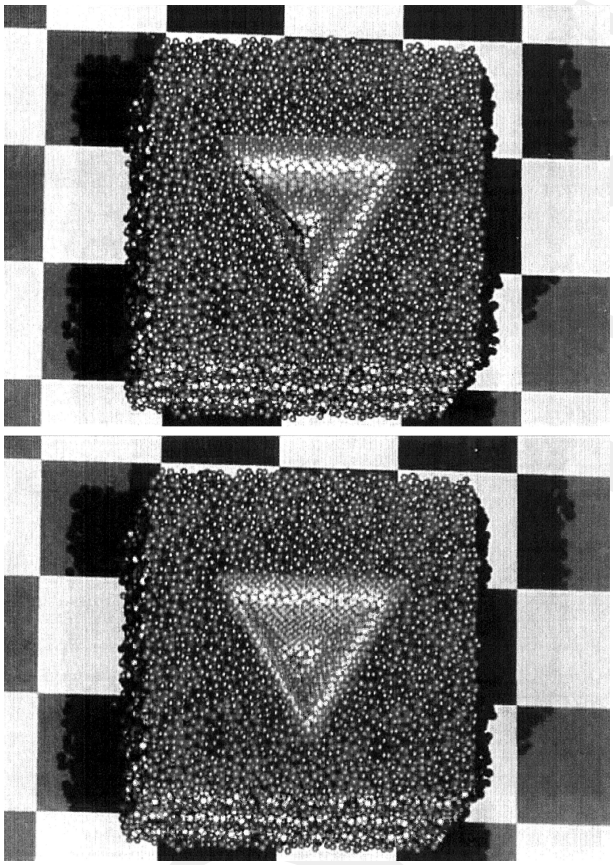

Figure 1. Indentation of silicon (as represented by the Stillinger-Weber potential) using thermostatted nonequilibrium molecular dynamics. Results were compared using two different types of tetrahedral indentors, one that was perfectly smooth, the other atomistic.

Few-particle systems, small enough for a thorough analysis of their phase-space distributions, were simulated too. This work was stimulated by Nosé's breakthrough of 1984 [3]. The phase-space structures the small-system simulations revealed were all multifractal, with the phase-space probability density singular everywhere, varying as a fractional power of separation. These wild nonequilibrium distributions are qualitatively unlike the smooth distributions known to Gibbs, Boltzmann, and to the generations of students of equilibrium statistical mechanics brought up on their ideas.

Consider the simple Galton-Board problem shown in figure 2. A mass point particle falls (under the effect of a fixed gravitational field) through a triangular-lattice array of scatterers. The dynamics is constrained to occur at fixed kinetic energy, by using Gauss' Principle. A sample nonequilibrium distribution, describing the collisions which occur in a nonequilibrium Galton Board, is also shown in figure 2 [6]. Each point in the figure indicates the location of a collision (on the abscissa) and the tangential velocity (the ordinate) for a mass point scattering from the array of hard scatterers. Evidently the distribution is *fractal* rather than continuous. The density

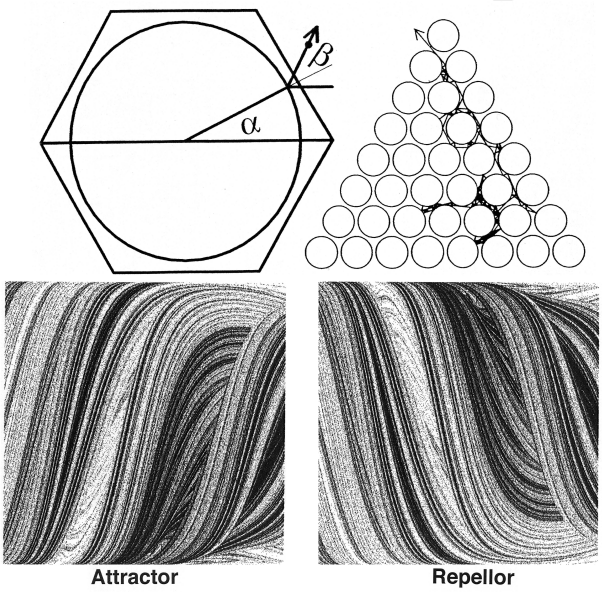

Figure 2. A finite portion of the Galton Board scattering system is shown at top right. Below is shown the phase plane for the Galton Board problem. The 10^6 attractor points $(\cos\alpha, \sin\beta)$ shown here represent one million successive collisions of a point particle in an *infinite* periodic array of hard-disk scatterers. This structure is a fractal "strange attractor". Its time-reversed cousin, the unobservable "even stranger repellor", is shown to the right. For details see [6].

of points varies as a *fractional* power of the separation everywhere in the distribution. At equilibrium, where the field vanishes and Gauss' constraint is unnecessary, the corresponding distribution of collisions would instead cover the plot smoothly and uniformly.

At first, the time-reversibility properties of these fractal distributions seemed paradoxical. For every trajectory going forward in time a reversed trajectory, with the coordinate frames played backwards, was also a solution of the motion equations. How could this symmetric situation be consistent with the Second Law of Thermodynamics, which restricts observable time developments to those for which entropy increases? We explore the details of the explanation for a simple mechanical model in section 5.

The resolution of (Loschmidt's) Reversibility Paradox using Nosé-Hoover mechanics is simplest for nonequilibrium steady states [1,7] such as the Galton Board problem discussed above. The phase-space flow in such cases invariably seeks out a fractal strange attractor. The dynamics on this attractor is (Lyapunov) *unstable* in the sense that two nearby points tend to separate, *exponentially* fast, in time. The attractor dynamics is *stable* in the sense that the flow contracts (on the average), eventually occupying *zero* phase volume! The corresponding phase-space density $f(q,p)$ is singular everywhere! The time-reversed version of the attractor dynamics (which defines the "repellor") has also reversed stability properties. In the neigh-

borhood of the repellor the time-averaged flow expands rather than contracts (on the average) and is, as a consequence, too unstable to be observed. In fact, the only way in which the unobservable phase-space repellors can be generated is by time-reversing the observed attractor states.

5. Example problem: nonequilibrium heat conducting oscillator

The concepts of fractal distributions, time-reversible irreversibility, and Lyapunov instability are all best assimilated through simple examples. The harmonic oscillator is arguably the *simplest* system with a smooth phase-space distribution. When Nosé-Hoover mechanics is applied to it the motion takes place in a three-dimensional (q, p, ζ) phase space:

$$\dot{q} = p/m, \qquad \dot{p} = -\kappa q - \zeta p, \qquad \dot{\zeta} = \left[(p^2/mkT) - 1 \right] / \tau^2.$$

These flow equations are consistent with Gibbs' canonical distribution for the oscillator:

$$f(q,p,\zeta) \propto f_q \times f_p \times f_\zeta \, ,$$

$$f_q = \exp\left(\frac{-\kappa q^2}{2kT} \right) \left(\frac{2\pi kT}{\kappa} \right)^{-1/2} ,$$

$$f_p = \exp\left(\frac{-p^2}{2mkT} \right) (2\pi mkT)^{-1/2} ,$$

$$f_\zeta = \exp\left(\frac{-\zeta^2 \tau_\zeta^2}{2} \right) \left(\frac{2\pi}{\tau_\zeta^2} \right)^{-1/2} .$$

Numerical investigation [8,9] showed that this system is not sufficiently mixing in phase space to access the full canonical distribution. The oscillator phase-space is broken up into infinitely-many noncommunicating regions. There is a "chaotic" region, in which nearby trajectories depart exponentially fast from one another. This exponential rate of trajectory separation is "Lyapunov instability", the defining feature of chaos. In addition to the unstable region there are an infinite number of noncommunicating stable regions. The lack of ergodicity in the model suggests that the Nosé-Hoover oscillator is not a good model for equilibrium statistical mechanics. The results obtained from it would depend upon the initial conditions.

On the other hand, adding a second control variable, to control also the *fourth* moment of the velocity distribution *does* achieve the full distribution [10]. The new set of differential equations,

$$\begin{aligned} \dot{q} &= p/m, \qquad \dot{p} = -\kappa q - \zeta p - \xi p (p^2/mkT), \\ \dot{\zeta} &= [(p^2/mkT) - 1]/\tau_\zeta^2, \\ \dot{\xi} &= [(p^2/mkT)^2 - 3(p^2/mkT)]/\tau_\xi^2 \end{aligned}$$

can readily be integrated using the fourth-order Runge-Kutta method. With a timestep of 0.001 the integration error that results is of the same order as the roundoff error in double-precision arithmentic. The distribution which results from these equilibrium equations of motion is again an extended canonical distribution:

$$f(q,p,\zeta,\xi) = f_q \times f_p \times f_\zeta \times f_\xi \,,$$

where the ξ distribution is also Gaussian:

$$f_\xi = \exp\left(-\xi^2\tau_\xi^2/2\right)\left(2\pi/\tau_\xi^2\right)^{-1/2}.$$

Figure 3 shows the time development of the distribution in the (q,p) and (ζ,ξ) subspaces of the phase space for the special case

$$m = k = T = 1, \qquad \tau_\zeta = \tau_\xi = 3.7.$$

The relaxation times are a little more than half the unconstrained oscillator period of 2π. Numerical investigations suggest that this oscillator accesses the entire phase space. The Lyapunov spectrum of exponents is

$$\{\lambda_{\rm eq}\} = \{+0.102, 0.000, 0.000, -0.102\}.$$

1 In this equilibrium case there is no strange attractor. The full phase space is explored by the motion, with the Gaussian distribution seen in figure 3.

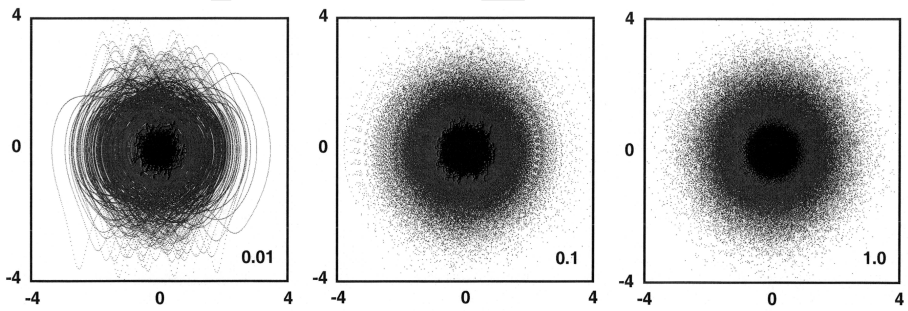

Figure 3. Development of the $\{q,p\}$ and $\{\zeta,\xi\}$ distribution functions at equilibrium, for the doubly-thermostatted oscillator. The final distribution is a Gaussian in all four variables, with the rms values of ζ and ξ smaller than those of q and p by a factor of $\tau = 3.7$ Each of the three plots shows 200,000 points. The time separations between successive points are 0.01, 0.10, and 1.0, where the Runge-Kutta timestep is 0.001.

2 A *nonequilibrium* version of the same oscillator can be achieved by making the temperature T a function of the coordinate q:

$$\frac{T}{T_0} = 1 + \epsilon \tanh\left(\frac{q}{h}\right).$$

In the special case

$$T_0 = \epsilon = h = 1, \qquad \tau_\zeta = \tau_\xi = 3.7,$$

the motion is the limit cycle shown in figure 4. The dimensionality of this limit-cycle attractor is unity, rather than four. The Lyapunov exponents for the limit cycle are

$$\{\lambda_{3.7,3.7}\} = \{0.000, -0.018, -0.079, -0.122\}.$$

The lack of any positive Lyapunov exponents indicates that the one-dimensional limit-cycle motion is completely stable.

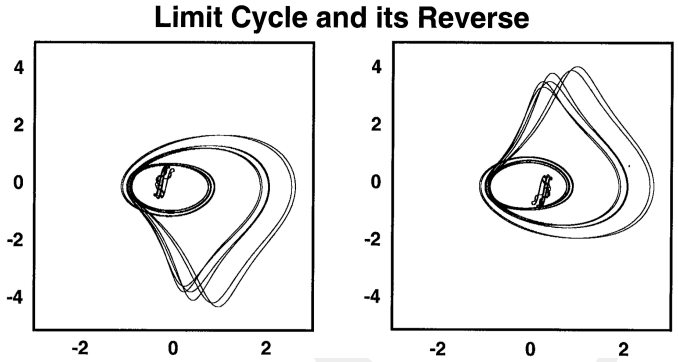

Figure 4. Limit cycle for the nonequilibrium oscillator with both thermostat variables set equal to 3.7. The reversed cycle is also shown. In both cases half a million points, separated by one thousand timesteps, are shown. (q, p) and (ζ, ξ) pairs of points are shown separately. The (ζ, ξ) pairs are those closer to the origin.

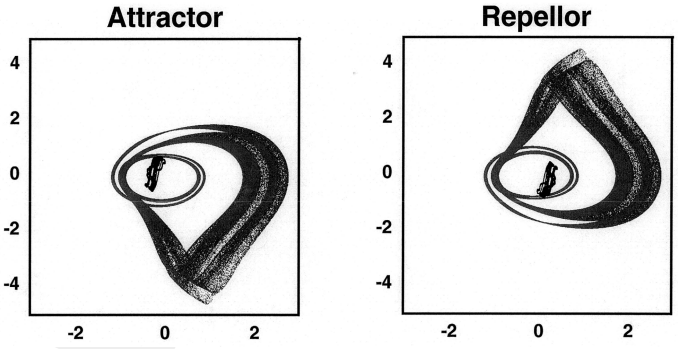

Figure 5. Strange attractor for the nonequilibrium oscillator with thermostat relaxation times $(\tau_\zeta, \tau_\xi) = (3.8, 3.6)$. The reversed attractor (the repellor) is also shown. In both cases half a million points, separated by one thousand timesteps, are shown.

The sum total of the Lyapunov exponents, -0.219, is the time-averaged rate-of-change of the comoving phase volume $\otimes$ in the neighborhood of the limit cycle:

$$\left\langle \frac{\mathrm{d}\ln\otimes}{\mathrm{d}t} \right\rangle = -\left\langle \frac{\mathrm{d}\ln f}{\mathrm{d}t} \right\rangle = \sum \lambda = -0.219.$$

The reversed motion, shown also in figure 4, has a reversed Lyapunov spectrum (with three positive exponents and no negative ones), and, though this motion is formally a solution of the motion equations, it is unobservable.

A slight change in the two thermostat relaxation times to

$$\tau_\zeta = 3.8, \qquad \tau_\xi = 3.6,$$

gives rise to the "strange attractor" shown in figure 5. The dimensionality of the attractor can be estimated from the Lyapunov spectrum

$$\{\lambda_{3.8,3.6}\} = \{+0.010, 0.000, -0.056, -0.159\}.$$

by using Kaplan and Yorke's conjecture that the dimension corresponds to the number of Lyapunov exponents whose sum is zero. Interpolating between the two-exponent sum and the three-exponent sum:

$$\lambda_1 + \lambda_2 = 0.010, \qquad \lambda_1 + \lambda_2 + \lambda_3 = -0.046,$$

gives a dimensionality of $D_{\mathrm{KY}} = 2 + 10/56 = 2.18$.

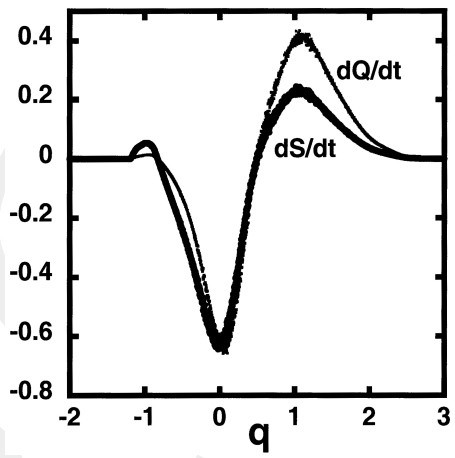

Figure 6. Histograms showing the densities of the time-averaged heat transfer $\langle \mathrm{d}Q/\mathrm{d}t \rangle$ (lighter curve) and entropy production $\langle \mathrm{d}S_{\mathrm{int}}/\mathrm{d}t \rangle$ (heavier curve) as functions of the oscillator coordinate q for the chaotic oscillator away from equilibrium. The total heat transfer is exactly zero while the entropy production is necessarily positive (for microscopic stability and for consistency with Clausius' form of the Second Law of Thermodynamics). Both total heat and total entropy production are obtained by integrating the densities shown with respect to the coordinate q.

In this model system the overall time-averaged heat transfer is zero, but, on the average, the heat is taken in at a higher temperature than that at which heat is extracted, corresponding to an entropy increase $\mathrm{d}S_{\mathrm{ext}}/\mathrm{d}t$ in the heat reservoirs interacting with the oscillator. Figure 6 shows the time-averaged distributions of $\langle \mathrm{d}Q/\mathrm{d}t \rangle$

and $\langle {\rm d}S_{\rm int}/{\rm d}t\rangle$ in space corresponding to the 2.18-dimensional strange attractor. The distributions for the limit cycle are scarcely different.

For either of the models, the total entropy change is

$$-\left\langle \frac{{\rm d}(S_{\rm ext}/k)}{{\rm d}t}\right\rangle = \left\langle \frac{{\rm d}(S_{\rm int}/k)}{{\rm d}t}\right\rangle = \left\langle \frac{({\rm d}Q/{\rm d}t)}{kT}\right\rangle$$
$$= \left\langle \left[-\zeta p - \xi \frac{p^2}{mkT} p \right] \frac{\dot q}{T} \right\rangle = \left\langle -\zeta - 3\xi \frac{p^2}{mkT} \right\rangle .$$

The last equality follows from two time averages:

$$\langle \zeta \dot\zeta \rangle \equiv 0 \to \left\langle \zeta \frac{p^2}{mkT} \right\rangle = \langle \zeta \rangle ,$$
$$\langle \xi \dot\xi \rangle \equiv 0 \to \left\langle \xi \left(\frac{p^2}{mkT} \right)^2 \right\rangle = \left\langle 3\xi \left(\frac{p^2}{mkT} \right) \right\rangle .$$

Notice that the time-averaged expression

$$\left\langle \frac{{\rm d}(S_{\rm ext}/k)}{{\rm d}t}\right\rangle = \left\langle \zeta + 3\xi \frac{p^2}{mkT} \right\rangle$$

is identically equal to the time-averaged rate at which the phase volume collapses onto the strange attractor:

$$-\left\langle \frac{{\rm d}\ln \otimes}{{\rm d}t}\right\rangle = \left\langle \frac{{\rm d}\ln f}{{\rm d}t}\right\rangle = -\left\langle \frac{\partial \dot q}{\partial q}\right\rangle - \left\langle \frac{\partial \dot p}{\partial p}\right\rangle - \left\langle \frac{\partial \dot\zeta}{\partial \zeta}\right\rangle - \left\langle \frac{\partial \dot\xi}{\partial \xi}\right\rangle$$
$$= 0 + \left\langle \zeta + 3\xi \frac{p^2}{mkT} \right\rangle + 0 + 0$$
$$\longrightarrow \left\langle \frac{{\rm d}(S_{\rm ext}/k)}{{\rm d}t}\right\rangle = -\left\langle \frac{{\rm d}(S_{\rm int}/k)}{{\rm d}t}\right\rangle = \left\langle \frac{{\rm d}\ln f}{{\rm d}t}\right\rangle$$
$$= \left\langle \zeta + 3\xi \frac{p^2}{mkT} \right\rangle = +0.205.$$

This correspondence is no coincidence. Here, as well as in the simpler Nosé-Hoover case, the time-rate-of-change of the phase volume (equivalent to the time-rate-of-change of the internal Gibbs' entropy in equilibrium statatistical mechanics) is *exactly* equal to the time-averaged rate of the external entropy increase in the heat reservoirs represented by the control variables ζ and ξ.

The Second Law statement that the overall entropy change in the external reservoirs must be positive is precisely equivalent to the microscopic statement that phase volume must collapse (onto an attractor) rather than diverge. Recall Clausius' form for the Second Law of Thermodynamics,

$$\oint \frac{1}{T} \frac{{\rm d}Q}{{\rm d}t}\, {\rm d}t' < 0,$$

where the integral is over any cyclic process which returns the system to its initial state, $(\mathrm{d}Q/\mathrm{d}t)$ is the rate at which heat is taken in by the system during the process, and T is the temperature of the reservoir with which the heat transfer takes place at the time t'. We see that the microscopic Second Law of Thermodynamics, from nonequilibrium molecular dynamics, has exactly Clausius' form, but with an additional averaging operation:

$$\left\langle \oint \frac{1}{kT} \, \frac{\mathrm{d}Q}{\mathrm{d}t} \right\rangle < 0.$$

In the microscopic case the average is over (many repetitions of) a nonequilibrium cyclic process. The requirement that the overall entropy increase (of the reservoirs!) be positive, is a direct consequence of the microscopic requirement that the occupied phase space cannot diverge in any stable microscopic nonequilibrium flow cycle.

Either by consciously violating Gauss' Principle of Least Constraint or by making an otherwise unwise choice of thermostat variables, the equivalence of the rate of microscopic phase-volume collapse with the rate of thermodynamic entropy increase, can be lost. For examples, see the references listed on Rainer Klages' website. It is evident that thermostats and nonequilibrium motion equations which maintain the equivalence of the dynamics with the Second Law are best. The zero-volume nature of the nonequilibrium attractors required for this stability also shows just how rare the nonequilibrium states are.

6. Conclusions

The same dynamical tools which solved the equilibrium many-body problem of statistical mechanics have been generalized to make possible the simulation of *nonequilibrium* problems. Velocity rescaling, Gauss' Principle of Least Constraint, and nonequilibrium Nosé-Hoover mechanics all lead to exactly the same form for the nonequilibrium motion equations,

$$\{\dot{p} = F - \zeta p\}.$$

Nosé-Hoover mechanics (and the generalization of it in the example detailed above) has also an intimate connection with the Second Law of Thermodynamics. Analyses of the strange attractors generated by that mechanics have shown that the irreversible Second Law has its roots in the chaotic nature of the time-reversible strange attractors generated by constrained flows. The microscopic version of the Second Law is the (time-averaged) statement that phase volume away from equilibrium must shrink (and ultimately vanish) rather than grow (and ultimately diverge).

Despite this new understanding there is considerable work yet to be done in characterizing the attractors. These are ideal problems for undergraduate and graduate research. The dimensionality of these small-system phase spaces is just right for the numerical investigation of Lyapunov Spectra, the various fractal dimensionalities, and conjectures like that proposed so long ago by Kaplan and Yorke.

This work was carried out under the auspices of the United States Department of Energy at the Lawrence Livermore National Laboratory under Contract W–7405–Eng–48.

References

1. Hoover Wm.G. Time Reversibility, Computer Simulation, and Chaos. World Scientific, Singapore, 1999 and 2001.
2. Hoover W.G. Computational Statistical Mechanics. Elsevier, New York, 1991.
3. Nosé S., J. Chem. Phys., 1984, **81**, 511.
4. Hoover Wm.G., J. Chem. Phys., 1998, **109**, 4164.
5. Kallman J.S., Hoover W.G., Hoover C.G., De Groot A.J., Lee S.M., Wooten F., Phys. Rev. B, 1993, **47**, 7705.
6. Moran B. , Hoover W.G., Bestiale S., J. Stat. Phys., 1987, **48**, 709.
7. Holian B.L., Hoover W.G., Posch H.A., Phys. Rev. Letts., 1987, **59**, 10.
8. Hoover W.G., Phys. Rev. A, 1985, **31**, 1685.
9. Posch H.A., Hoover W.G., Vesely F.J., Phys. Rev. A, 1986, **33**, 4253.
10. Hoover Wm.G., Holian B.L., Phys. Lett. A, 1996, **211**, 253.